Algorithmic reconstruction of complete axonal arborizations in rat hippocampal neurons

Ruggero Scorcioni[1], Giorgio A Ascoli[1,2 *]

[1]Krasnow Institute for Advanced Study, George Mason University, Fairfax, VA 22030

[2]Psychology Department, George Mason University, Fairfax, VA 22030

* Corresponding author (ascoli@gmu.edu)

Abstract

Three-dimensional axonal morphologies are not currently available to the neuroscience community in a format suitable for computational modeling. We have designed an algorithm to reconstruct full axonal arborizations based on sets of digitized segments extracted from raw anatomical preparations. We applied this algorithm to eight rat neurons covering the entire synaptic loop of the hippocampal formation (entorhinal cortex, dentate gyrus, CA3, CA1, and subiculum). Since no digital reconstructions of axons have been previously completed for these cell classes, we validated the algorithm by comparing the resulting dendritic arborizations (which were automatically reconstructed along the axons) of the CA1 cells with those available in several public archives. The eight axonal morphologies are quantitatively analyzed and freely distributed in SWC format (http://www.krasnow.gmu.edu/L-Neuron).

Introduction

Complete three-dimensional reconstructions of neuronal dendrites are commonly used in computational neuroscience to develop anatomically accurate biophysical models of electrophysiology (e.g. [1,2]). Several hundreds dendritic reconstructions are publicly available in digital format through internet-based archives (e.g. [3,4]). In contrast, complete axonal morphologies are not readily available, in part because of the enormously laborious effort of semi-manual reconstruction. Digitized axonal arborizations in a format suitable for compartmental modeling would undoubtedly constitute a welcome addition to the electronic libraries of computational neuroanatomy.

The axonal anatomy of a tantalizing set of neurons from all regions of the rat hippocampal formation has been quantitatively characterized by Tamamaki and coworkers in the last 15 years [5-8]. The raw data on which these studies are based consist of classic camera lucida tracings of three CA1 pyramidal cells (one each from subfields CA1a, b, and c), one CA2 and one CA3 pyramidal cells, a dentate granule cell, an entorhinal (layer II) spiny stellate cell, and a projecting subicular neuron (SUB). The authors of these studies have digitized the drawings with computer-interfaced tablets [8] and have kindly provided us with the entire resulting dataset. These files represent a large and valuable source of information, but cannot be used for computational modeling or full quantitative morphometric analysis, as they contain lists of disjointed dendritic, axonal, and tissue contour segments.

In this paper we present a novel algorithm to recover fully connected axonal and dendritic trees from such lists of disjoint segments. Morphometric measurements are extracted from the dendritic trees to validate the method, and from the axons to provide

the first quantitative, cellular-level, comparative analysis among all known projecting fibers of the hippocampal formation. The final SWC files are made available through the internet (www.krasnow.gmu.edu/L-Neuron).

Materials and Methods

The Tamamaki dataset includes 8 neurons traced from male albino Sprague-Dawley rats. Each cell is described by a collection of digital files corresponding to the tissue slices, sectioned at a thickness of 0.065 mm. Each file includes a list of disjoint segments consisting of series of connected points. Each point is described by the X and Y coordinates on the slice, the slice number ("Z" coordinate), a numerical marker for segment origins and endings, and a type tag identifying the cell layer, hippocampal contours, dendrites, thick axons, and thin axons.

The algorithm to recover the structure of the neuronal trees converts the list of segments forming the neuronal trees into a fully connected binary structure in SWC format [3,4]. The algorithm is based on the following series of consecutive steps:

1) Compute the three-dimensional distance for each pair p_1,p_2 of points that satisfy the following constrains:
    a) they must belong to different segments (to avoid creation of branch loops)
    b) their eventual joining cannot lead to a trifurcation
2) Sort each pair by distance and consider all pairs below a given distance threshold T. Pairs within this set are moved to form a pair-pool PP if they simultaneously satisfy the following conditions:
    i) p_1 is the closest point to p_2
    ii) p_2 is the closest point to p_1

In a simple one-dimensional example, consider three points A=0.2, B=0.7, and C=0.9. While the closest point to A is B, the closest point to B is C. Thus, A and B would not be moved in PP. In contrast, B and C satisfy both (i) and (ii) and would thus be moved in PP.

3) Join each pair from PP by adding an extra segment p_1-p_2 thus reducing the total number of segments by one after each joining
4) Repeat steps 1 to 3 until only one segment is left. At each iteration increase the threshold T by 10% (the initial value was set to 0.001mm).

Since the Z coordinate is the same for all points within each slice (i.e., the Z position is "quantized"), the standard Euclidian distance between two points was substituted with the following formula for each pair of points on the same slice:

$$D=\sqrt{(X_1 - X_2)^2 + (Y_1 - Y_2)^2 + (0.33 \cdot 0.065)^2}$$

The 0.33 correction factor represents the average distance of two random points uniformly distributed in the range [-0.5,0.5], while 0.065 mm is the slice thickness. Note that this simple method of treating the Z coordinate is far less sophisticated than that based on cubic polynomials, introduced by Wolf et al. (1995) [9]. While the Wolf et al. method ensures greater precision and was successfully used for dendritic reconstructions [10], an error of the order of ~20 μm (0.33*65) is acceptable for reconstructions of projections axons, which typically span a space of several millimeters.

At the end of this phase, which is carried out on dendrites and axons separately (and disregarding the tissue contour data), the neuronal structure is stored as an intricate series of connected segments S. To provide the correct SWC output, an approximated position of the soma P needs to be derived. This position P was empirically determined

from a graphical representation of the original data based on the cell layer marker in the file, the indicated location in the original publication, and the surrounding dendritic shapes (e.g. for pyramidal cells, the soma lies between the basal and apical trees). The graphical package used for visualization is 3D Deep Exploration from Right Hemisphere (http://www.righthemisphere.com). The soma is defined as the closest point of S to P. The structure S is then reordered starting from the identified soma, completed with approximate diameter values (dendrites, 0.6 μm, thick axons, 0.4 μm, thin axons, 0.2 μm), and the final SWC output file is produced.

A graphical example of the algorithmically reconstructed axonal and dendritic trees of Tamamaki's cell CA1c is shown in Fig 1. The arrow points to a zoom-in on the corresponding dendritic trees. Fig 2 shows a thumbnail view of the other seven neurons.

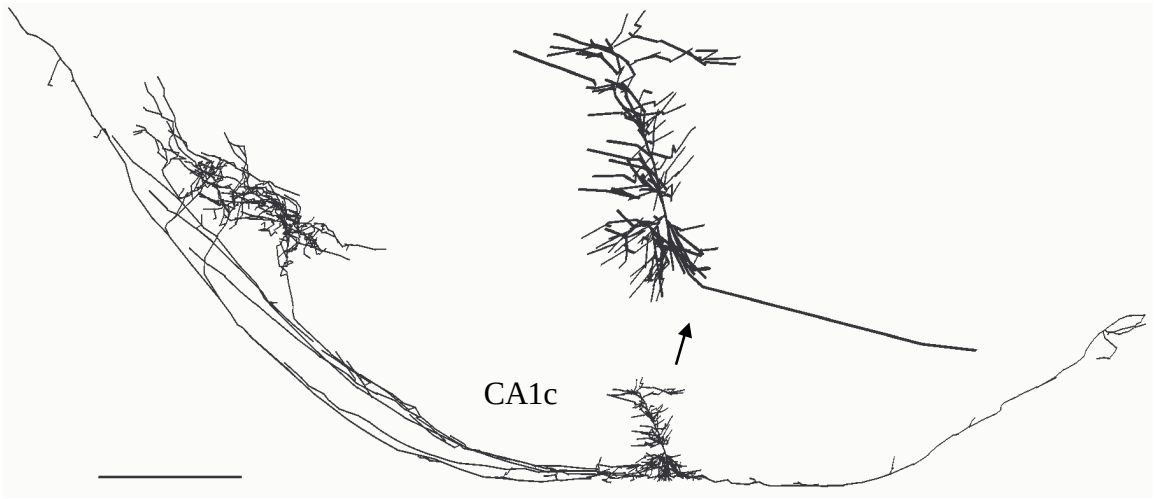

Fig 1: Recovered axonal and dendritic trees of CA1c with zoom-in on dendritic trees only. Bar = 1 mm (0.35mm for zoom-in)

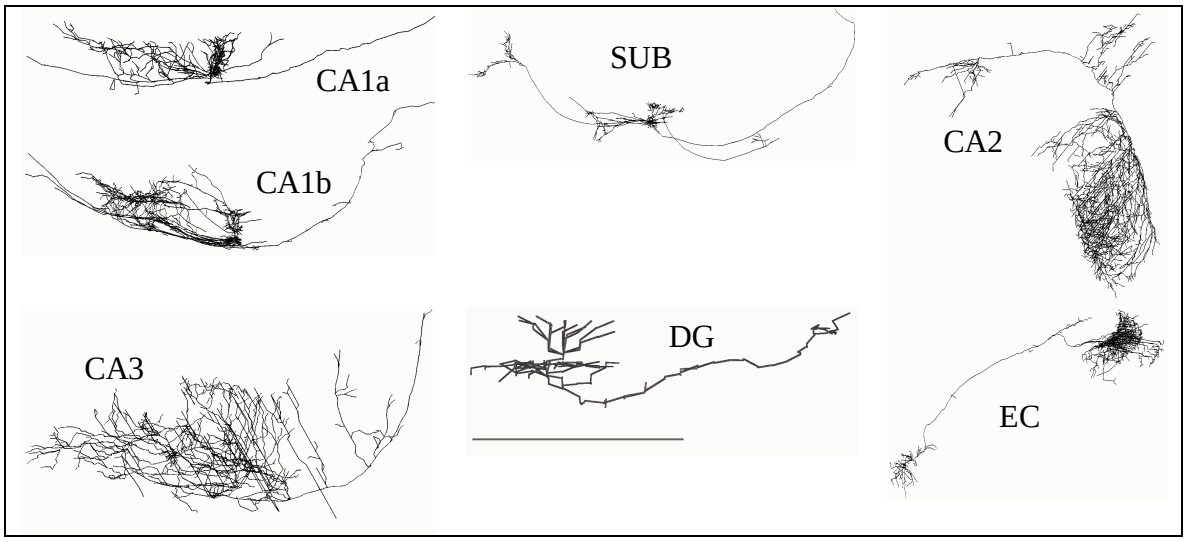

Fig 2: 2D views of the reconstructed neurons. Bar: CA1a: 2.8mm; CA1b: 4.3mm; CA3:3.2mm; SUB:4.6mm; DG: 1mm; CA2: 7.8mm; EC: 4.7mm

Algorithm Validation

To assess the accuracy of the reconstruction algorithm, we compared the dendritic morphologies of the three CA1 cells to those of a set of 78 CA1 neurons from four different laboratories [1,11-14]. This set provides a fair sample of the morphological variability among various available digital archives of hippocampal neuroanatomy [2]. We measured the number of bifurcations, number of terminal tips, and average branch order, and plotted each parameter against the relative distance along the path from the soma (Fig 3).

For each plot, the dashed lines represent the 78-neuron average plus and minus one standard deviation. Different markers correspond to different neurons: triangles for CA1a, squares for CA1b and circles for CA1c. In all three cases the variability of the reconstructed neurons is generally within one standard deviation. Thus, the neurons obtained with the algorithm described above are statistically within the morphological range of neurons reconstructed with standard techniques.

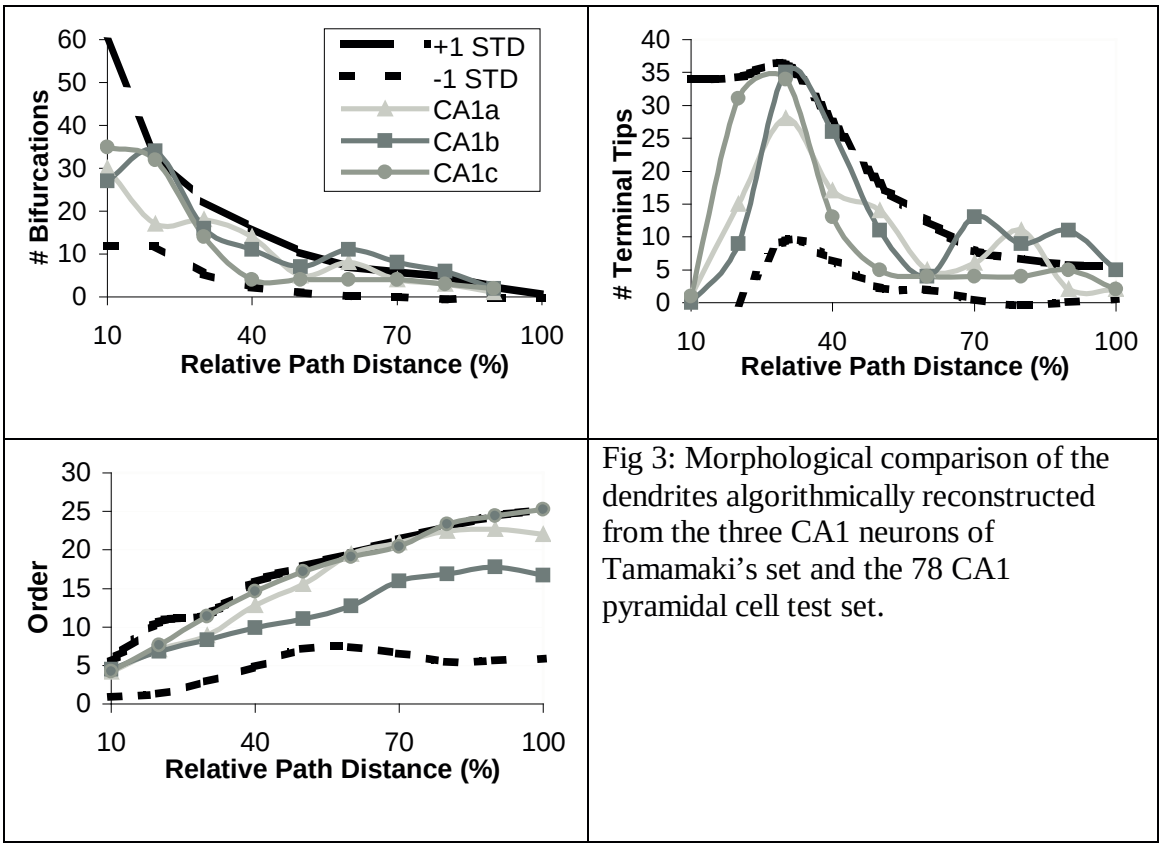

Fig 3: Morphological comparison of the dendrites algorithmically reconstructed from the three CA1 neurons of Tamamaki's set and the 78 CA1 pyramidal cell test set.

Axonal Analysis

The joining algorithm was applied to all 8 available neurons. Table 1 summarizes several common morphometric measurements from all axonal trees. The smallest axonal tree belongs to the dentate gyrus granule cell (DG), with only 35 bifurcations and a total length of 9.24 mm. In contrast, the longest axonal tree belongs to the CA2 pyramidal cell, with includes 975 bifurcations (more than 27 times the granule cell), and a total length of 423 mm (45 times longer than the granule cell). The maximum path distance, maximum branch order, and topological asymmetry all discriminated the most between the granule cell at the lower end and the CA1c pyramidal cell at the opposite end, but within a more

contained range of values. In comparison, the branch length average is fairly constant to 0.184 mm ±0.05.

Table 1: Morphometric summary of axonal trees from 8 different neurons of the hippocampal formation. See [2] for formal definitions of these parameters.

	# Bifurcations	Total Length (mm)	Max Euclidean Distance (mm)	Max Path Distance (mm)	Max Branch Order	Average Branch Length (mm)	Asymmetry
CA1a	138	51.4	3.11	4.44	25	0.187	0.617
CA1b	279	113	4.77	10.4	42	0.203	0.649
CA1c	252	79.0	5.11	15.6	73	0.157	0.672
CA2	975	423	7.01	13.6	60	0.217	0.644
CA3	391	206	4.95	7.68	33	0.263	0.584
EC	763	161	7.16	13.8	68	0.106	0.628
DG	35	9.24	1.50	3.47	17	0.134	0.574
SUB	149	61.6	8.68	13.8	26	0.207	0.614

A distribution analysis was also performed on the axonal trees of all eight neurons. In this case, the number of bifurcations and branch order are plotted against absolute path distance (Fig. 4). All plots follow a standard bell-shaped distribution. However, a marked difference is observed in the peak of bifurcation vs distance from the soma for all neurons. Interestingly, the corresponding positions appear to be almost proportional to the maximum path values (Table 1). The plots of branch order vs. path distance, in contrast, follow nearly linear trends, with considerable differences in slope among groups of neuronal classes (i.e. among panels in Fig. 4), and some intriguing grouping (within panels) despite obvious variation in maximum path length.

Conclusions

In this paper we present a novel and simple algorithm for the joining of disconnected segments. This algorithm allowed the reconstruction of complete axonal (and dendritic)

trees from all the principal cells of the hippocampal formation. The algorithm was only validated indirectly, by comparing dendritic morphometrics to population statistics of available data from the same classes. Unfortunately, a stronger comparison based on the application of an established method (see e.g. [9]) on the same axons is not applicable to the present data set. Given the relative ease of acquisition of camera lucida tracings (compared to semi-automated digital reconstructions), this algorithm holds the promise to generate a vast amount of axonal data in a format suitable for quantitative analysis and computational modeling.

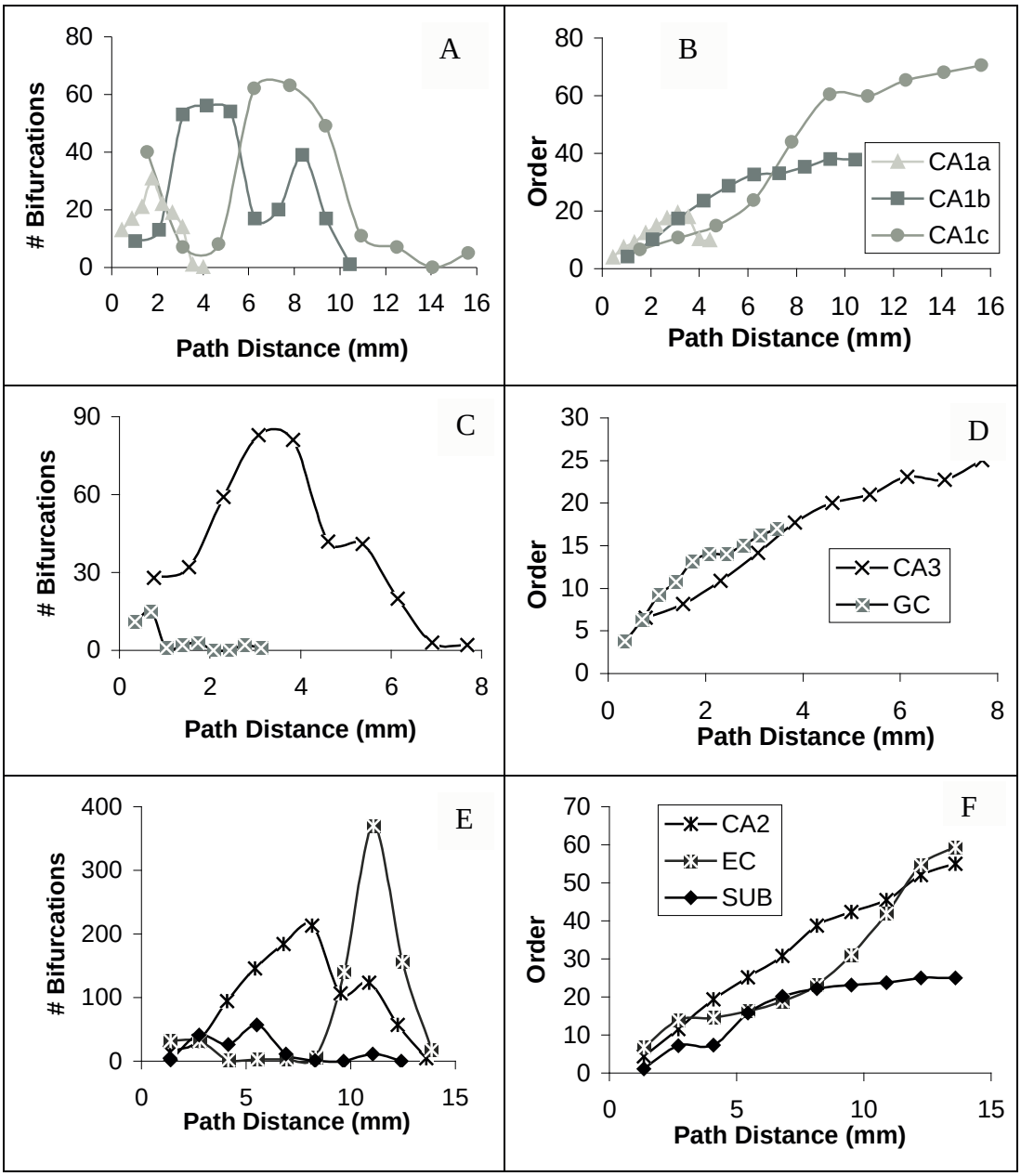

Fig 4: Axonal distributions of the number of bifurcations and branch order vs absolute path distance for all eight neurons.

References

[1] N.T. Carnevale, K.Y. Tsai, B.J. Claiborne, T.H. Brown, Comparative electrotonic analysis of three classes of rat hippocampal neurons. J. Neurophysiol. 78 (1997) 703-720

[2] R. Scorcioni, M.T. Lazarewicz, G.A. Ascoli, Quantitative morphometry of reconstructed hippocampal pyramidal cells: Differences between anatomical subregions and reconstructing laboratories. J. Comp. Neurol. 473(2) (2004) 177-193.

[3] R.C. Cannon, D.A. Turner, G.K. Pyapali, H.V. Wheal, An on-line archive of reconstructed hippocampal neurons. J. Neurosci. Methods 84 (1998) 49-54.

[4] G.A. Ascoli, J. Krichmar, S. Nasuto, S. Senft: Generation, description and storage of dendritic morphology data. Phil. Trans. R. Soc. B, 356(1412) (2001) 1131-1145

[5] N. Tamamaki, Y. Nojyo, Disposition of the slab-like modules formed by axon branches originating from single CA1 pyramidal neurons in the rat hippocampus. J. Comp. Neurol. 291(4) (1990) 509-519

[6] N. Tamamaki, Y. Nojyo, Crossing fiber arrays in the rat Hippocampus as demonstrated by three-dimensional reconstruction. J. Comp. Neurol. 303(3) (1991) 435-442

[7] N. Tamamaki, Y. Nojyo, Projection of the Entorhinal layer II neurons in the rat as revealed by intracellular pressure-injection of neurobiotin. Hippocampus 3 (1993) 471-480.

[8] N. Tamamaki, K. Abe, Y. Nojyo, Three-dimensional analysis of the whole axonal arbors originating from single CA2 pyramidal neurons in the rat hippocampus with the aid of a computer graphic technique. Brain Res. 452(1-2) (1988) 255-272.

[9] E. Wolf, A. Birinyi and S. Pomahazi, A fast 3-dimensional neuronal tree reconstruction system that uses cubic polynomials to estimate dendritic curvature J. Neurosci. Meth. 63 (1995) 137-145

[10] A.I. Gulyás, M. Megías, Z. Emri, and T. F. Freund, Total number and ratio of excitatory and inhibitory synapses converging onto single interneurons of different types in the CA1 area of the rat hippocampus, J. Neurosci. 19 (1999) 10082-10097.

[11] N. Ishisuka, W.M. Cowan, D.G. Amaral, A Quantitative analysis of the dendritic organization of pyramidal cells in the rat Hippocampus. J. Comp. Neurol. 362 (1995) 17-45

[12] M. Megias, Z. Emri, T.F. Freund, A.I. Gulyas, Total number and distribution of inhibitory and excitatory synapses on hippocampal CA1 pyramidal cells. Neuroscience. 102(3) (2001) 527-540.

[13] G.K. Pyapali, D.A. Turner, Increased dendritic extent in hippocampal CA1 neurons from aged F344 rats. Neurobiol. Aging 17 (1996) 601-611.

[14] G.K. Pyapali, A. Sik, M. Penttonen, G. Buzsaki, D.A. Turner, Dendritic properties of hippocampal CA1 pyramidal neurons in the rat: intracellular staining in vivo and in vitro. J. Comp. Neurol. 391 (1998) 335-352